Available online at www.sciencedirect.com
SCIENCE DIRECT®
Journal of the European Ceramic Society 25 (2005) 1789–1796
www.elsevier.com/locate/jeurceramsoc

Oxidation behaviour of an aluminium nitride–hafnium diboride ceramic composite

Davide Mattia[a,*], Martine Desmaison-Brut[a], Svetlana Dimovski[b], Yury Gogotsi[b], Jean Desmaison[a]

[a] *SPCTS, UMR-CNRS 6638, Université de Limoges, 123, av. A. Thomas, 87060 Limoges, France*
[b] *Department of Material Science and Engineering and A.J. Drexel Nanotechnology Institute, Drexel University, 3141 Chestnut Street, Philadelphia, PA 19104, USA*

Available online 21 January 2005

Abstract

An aluminium nitride–hafnium diboride electroconductive particulate composite was produced via hot isostatic pressing without sintering aids. Oxidation kinetics studies were performed up to 1350 °C under a flow of pure oxygen using a microbalance. The reaction products were analysed using SEM and XRD techniques. This composite had a high oxidation resistance up to 1200 °C. The kinetic curves had an asymptotic or paralinear shape. The formation of a protective oxide scale containing hafnia (HfO_2) and aluminium borate ($Al_{18}B_4O_{33}$) phases embedded in a glassy phase was observed. The evaporation of B_2O_3 was limited by the formation of refractory aluminium borate. Above 1200 °C, morphological observations showed the formation of a Maltese cross structure associated with the cracking of the oxide scale along the edges resulting in sigmoidal oxidation kinetics and in a high oxidation rate of the ceramic composite.

Keywords: Aluminium nitride; Hafnium diboride; Aluminium borate; Particulate composite; Oxidation kinetics

1. Introduction

Non-oxide ceramics represent a wide family of materials intensively studied in the last years in the search for better high temperature oxidation resistance and mechanical properties. Boron-containing ceramics, such as TiB_2, ZrB_2 and HfB_2 possess good mechanical properties as well as electroconductivity which enables electrical discharge machining (EDM).[1,2] This cutting/shaping technique is particularly suitable for materials with high hardness values.

Considering the oxidation behaviour, the high reactivity of these ceramics with oxygen and the low melting and boiling points of boron oxide yield the formation of thick TiB_2, ZrB_2, HfB_2 scales and an significant loss of material via evaporation of B_2O_3.[3]

In order to prevent boron oxide evaporation, which reduces the oxidation resistance of boride monolithic ceramics, composites in which the boron-containing ceramic is blended with silicon and/or aluminium-rich ceramic have been developed. Oxidation leads to the formation of SiO_2– and/or Al_2O_3–B_2O_3 glass, limiting the evaporation of boron oxide, and improve the oxidation resistance of the material.[4–8]

Concerning ceramic composites formed by aluminium nitride and borides of IVB-column metals, the oxidation behaviour of AlN–ZrB_2[9] and AlN–TiB_2[10] has been studied. In the former, a good oxidation resistance up to 1400 °C was observed with parabolic kinetics and the formation of aluminium borate crystals, $Al_{18}B_4O_{33}$, with columnar morphology.[9] In the latter, a similar kinetic behaviour was accompanied by higher mass gains as a result of formation of hollow aluminium borate crystals, which enhanced oxygen diffusion to the core.[10]

The objective of this work was to investigate the oxidation behaviour of a fully dense aluminium nitride-based composite with hafnium diboride as secondary phase.

* Corresponding author. Present address: Drexel University, Materials Science and Engineering Department and A.J. Drexel Nanotechnology Institute, Room CAT 383, 3141 Chestnut Street, 19104 Philadelphia, PA, USA. Tel.: +1 215 895 2382; fax: +1 215 895 6760.
E-mail address: davide.mattia@drexel.edu (D. Mattia).

0955-2219/$ – see front matter © 2004 Elsevier Ltd. All rights reserved.
doi:10.1016/j.jeurceramsoc.2004.12.011

2. Experimental procedure

The starting powders, aluminium nitride grade D (H.C. Stark, Germany) and hafnium diboride (Cerac, Milwaukee, WI), in a 73:27 vol.% (79:21 mol%) proportion, were mixed in anhydrous ether for 24 h in a Turbula mixer. The obtained powder mixture was then dried up at 60 °C under vacuum, sieved (32 μm) and cold isostatically pressed at 200 MPa for 120 s. The green body was sealed in a silica glass container with a BN layer as protective barrier, degassed for 24 h at 500 °C and hipped (ACB Alstom Atlantique press) at 1860 °C and 170 MPa. The resulting ceramic, fully densified ($\rho_{rel} > 99\%$), was then cut in cubes of 4 mm side and polished using SiC paper 4000.

Isothermal oxidation tests were performed with a Setaram microbalance at temperatures up to 1350 °C in flowing oxygen (10 l/h). To avoid oxidation during the heating of the furnace, the sample was kept in the cold zone under argon flow. At the test temperature, argon was replaced by oxygen and the sample was lowered into the hot zone. Non-isothermal tests were performed in flowing oxygen (10 l/h) with a 1.5 °C/min heating rate up to 1425 °C. At the end of the runs, the specimens were rapidly raised to avoid further oxidation during cooling.

The oxidized cubes were analysed by X-ray diffraction (Siemens D5000 diffractometer) and SEM (Philips XL30 coupled with an EDAX 9100/60 EDS analyser). Electron probe microanalysis (EPMA-WDX) was performed with a JEOL 8900 RL superprobe.[11]

3. Results

3.1. Oxidation kinetics

The composite starts to oxidize above 800 °C and shows a very low mass gain up to 1350 °C, above which a sharp increase for oxidation rate occurs (Fig. 1).

Isothermal oxidation kinetic curves were plotted as mass variation per surface area versus time. Experiments were conducted for 24 h in the 1000–1200 °C (Fig. 2) and 1225–1350 °C (Fig. 3) temperature ranges. The shape of kinetic curves changes as a function of temperature. The kinetic are logarithmic[12] up to 1100 °C, while at 1200 °C after an initial step a kinetic break is observed leading to a linear kinetic. Above 1225 °C, they are becoming sigmoidal as demonstrated by the mass gains of samples oxidised for 2, 4, 6, 10, 13 and 24 h at 1300 °C (Fig. 4).

3.2. Phase characterization and morphology of the oxidized samples

XRD patterns of the surface of samples oxidized in the 1000–1200 °C temperature range are shown in Fig. 5. At 1000 °C, HfO_2 peaks appear along with HfB_2 and AlN ones,

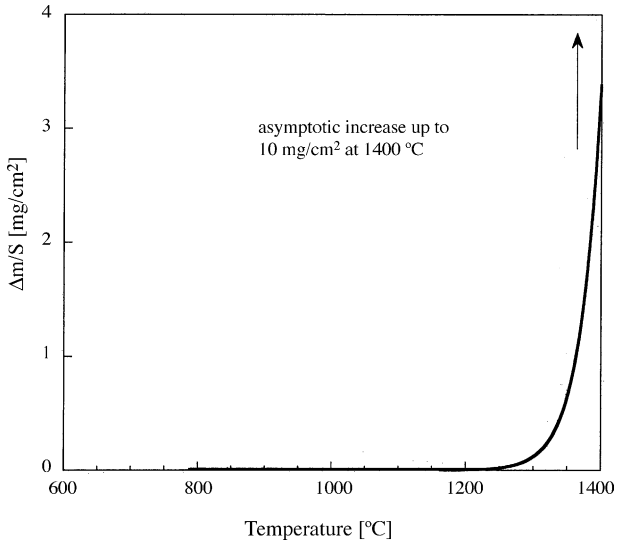

Fig. 1. Non-isothermal curve in flowing oxygen, 2 °C/min ramp.

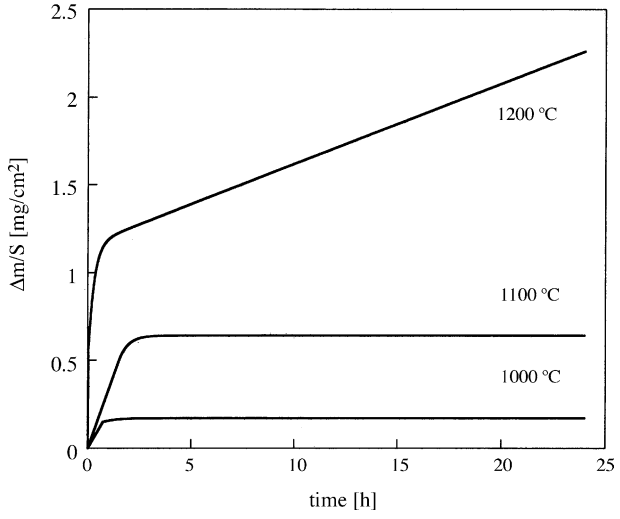

Fig. 2. Isothermal kinetic curves obtained between 1000 and 1200 °C.

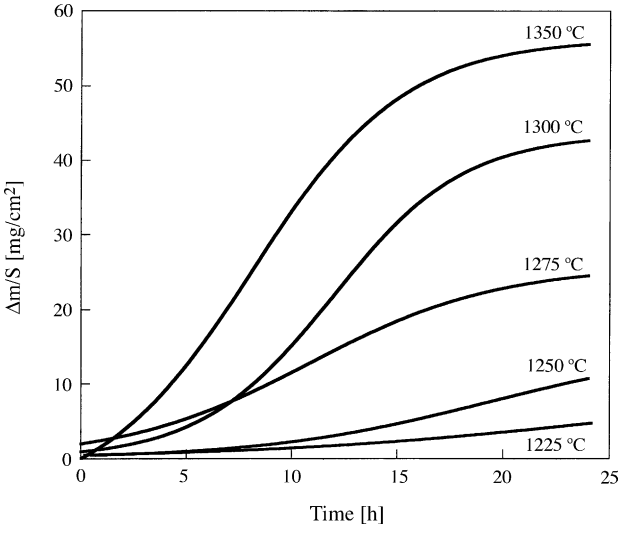

Fig. 3. Isothermal kinetic curves on the temperature range 1225–1350 °C.

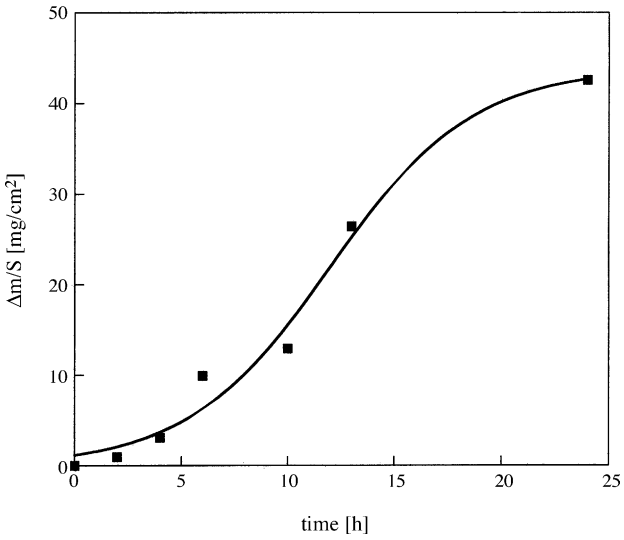

Fig. 4. Mass gain at 1300 °C for 2, 4, 6, 10, 13 and 24 h showing the sigmoid kinetic shape.

the latter being no more visible over 1100 °C. Aluminium borate peaks appear only at 1200 °C, where only the former and HfO_2 peaks are still visible. XRD analysis of samples oxidized at higher temperatures showed no significant difference from those at 1200 °C.

The surface of samples treated at 1000 °C for 24 h appears to be covered by a glassy phase (Fig. 6). EDS analysis of the surface of a sample oxidised at 1200 °C for 24 h shows the presence of hafnium oxide grains, some of them being embedded in a glassy phase, which appears to be composed of aluminium and oxygen, boron being not detectable by the apparatus (Fig. 7).

Intense oxidation for temperatures above 1200 °C led to the formation of a so-called Maltese cross structure, a cross section of which is shown in Fig. 8, while the inset shows the overall dimensions. The opening of the scale at the cubes' edges corresponds to the inflexion point on the kinetic curves, which shifts towards shorter oxidation times with increasing temperature (Fig. 3).

Table 1
EPMA-WDS analysis for a sample oxidised at 1300 °C: mean and standard values over five analysis

Phase	Element (wt.%)				Total
	B	Al	O	Hf	
Al borate	2.8 ± 0.2	44.3 ± 0.6	51.3 ± 1.4	0.0	98.3 ± 1.1
Hafnia	0	<1%	17.5 ± 1.6	75.8 ± 0.8	94.4 ± 1.7

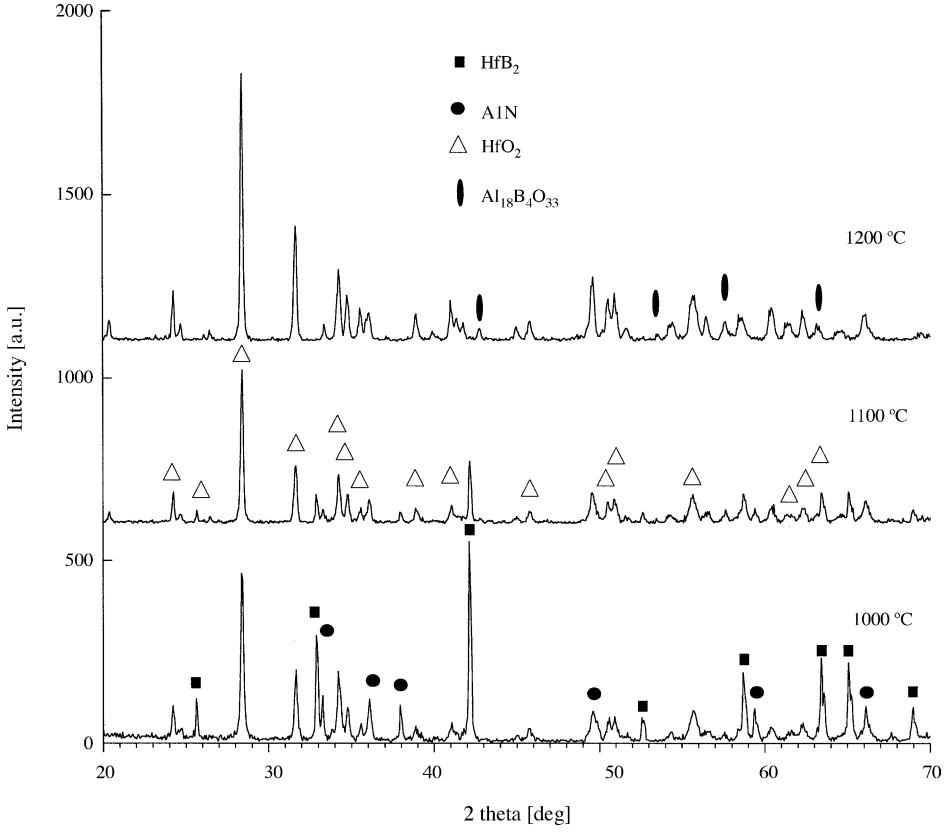

Fig. 5. XRD patterns of oxidized samples after 24 h oxidation at 1000–1200 °C.

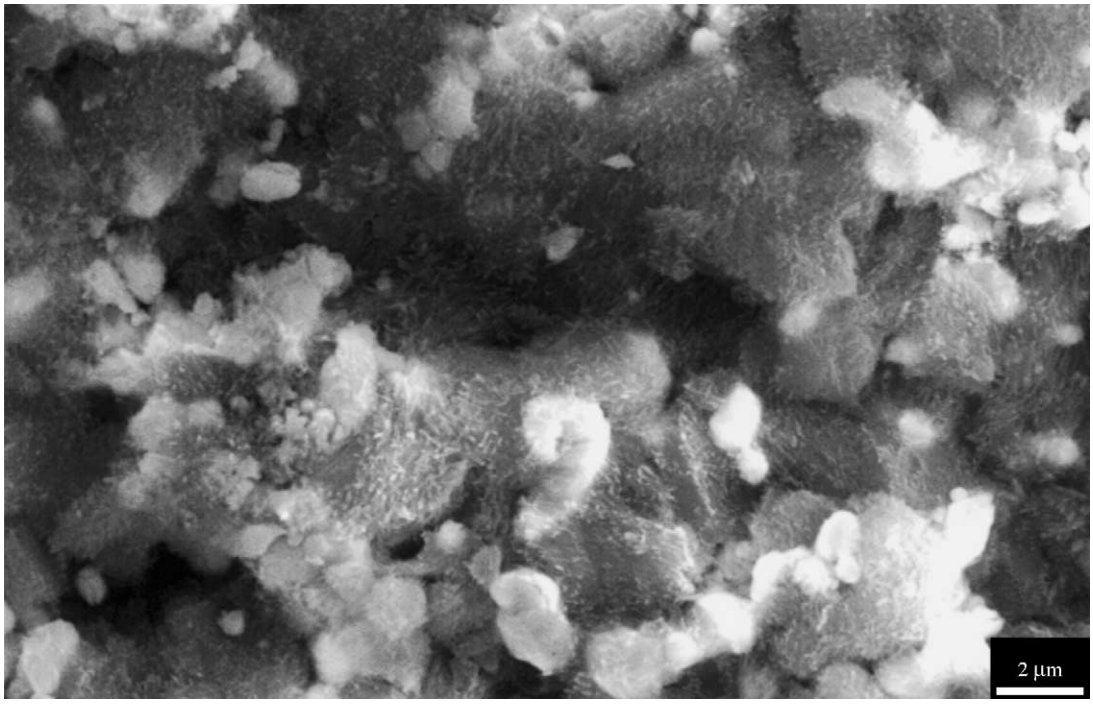

Fig. 6. SEM image of the oxidized surface, 24 h at 1000 °C, showing a glassy phase covering the surface.

Boron detection was made possible using the EPMA-WDS technique. Electron probe microanalyses were performed on the cross section of samples oxidized for 24 h at different temperatures. Results for 1300 °C are reported in Table 1.

The quantitative values reported in Table 1 can be considered acceptable even though the total is slightly less than 100%. The small deviation may be due to the limiting diameter of the aluminium borate grains, which approaches the microprobe's resolution, and to the geometry of hafnia grains.

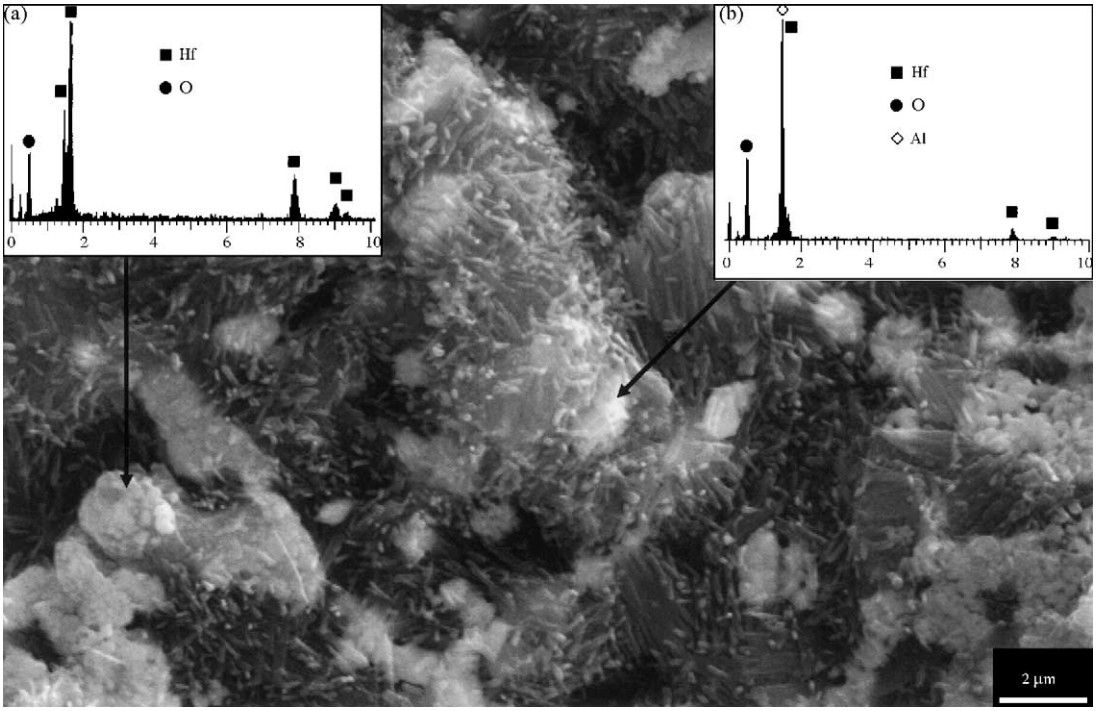

Fig. 7. SEM image of the oxidized surface, 24 h at 1200 °C and EDS spectra showing (a) HfO_2 grains and (b) HfO_2 grains covered by an Al-based glassy phase.

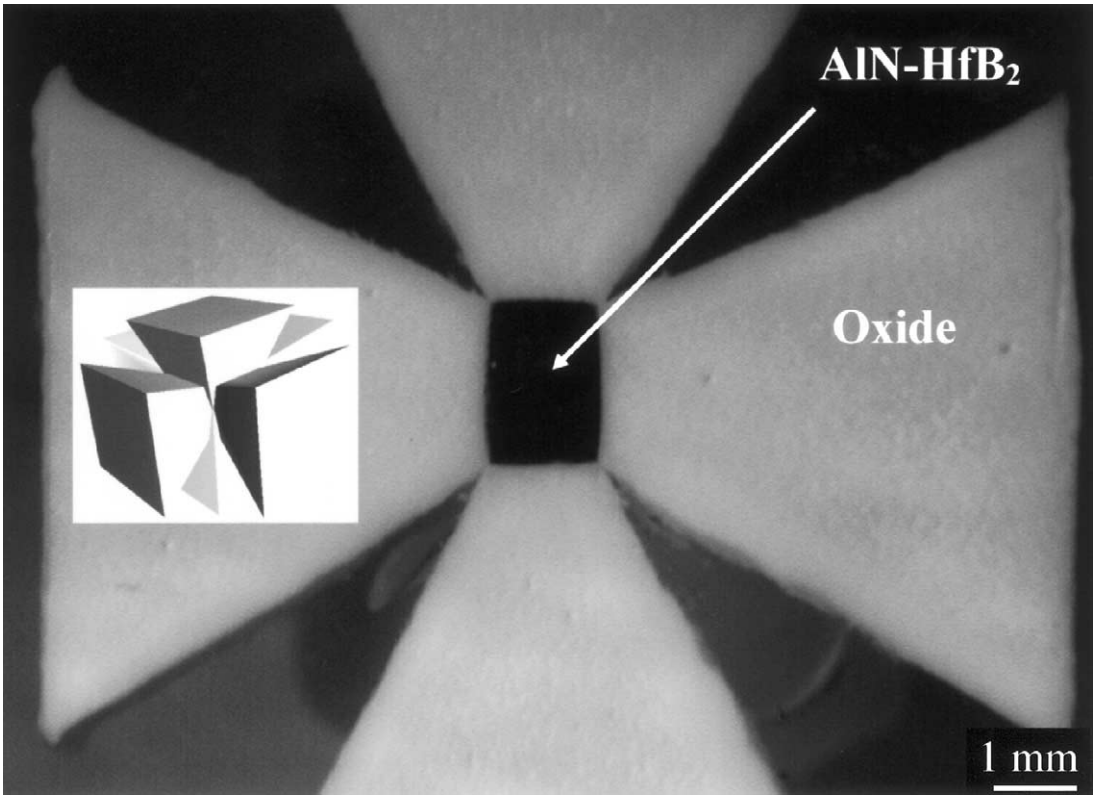

Fig. 8. Optical image of the cross section of an oxidized sample, 24 h at 1350 °C, forming a Maltese cross structure.

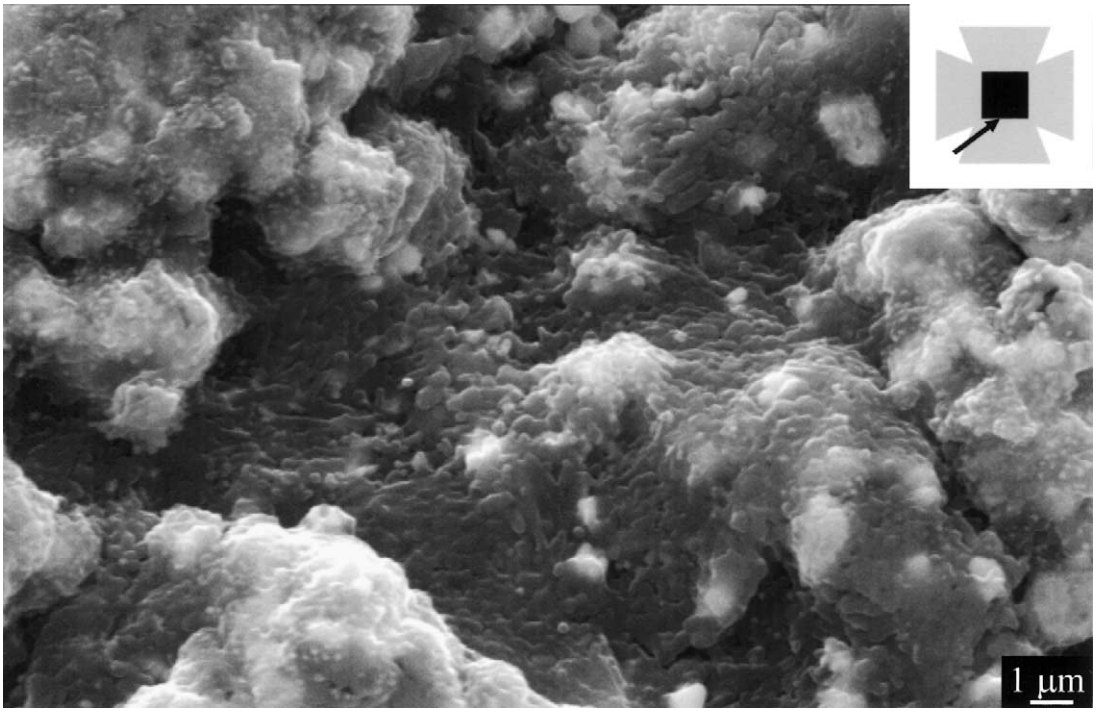

Fig. 9. SEM micrograph of the cross side near the non-oxidized bulk, 24 h at 1350 °C.

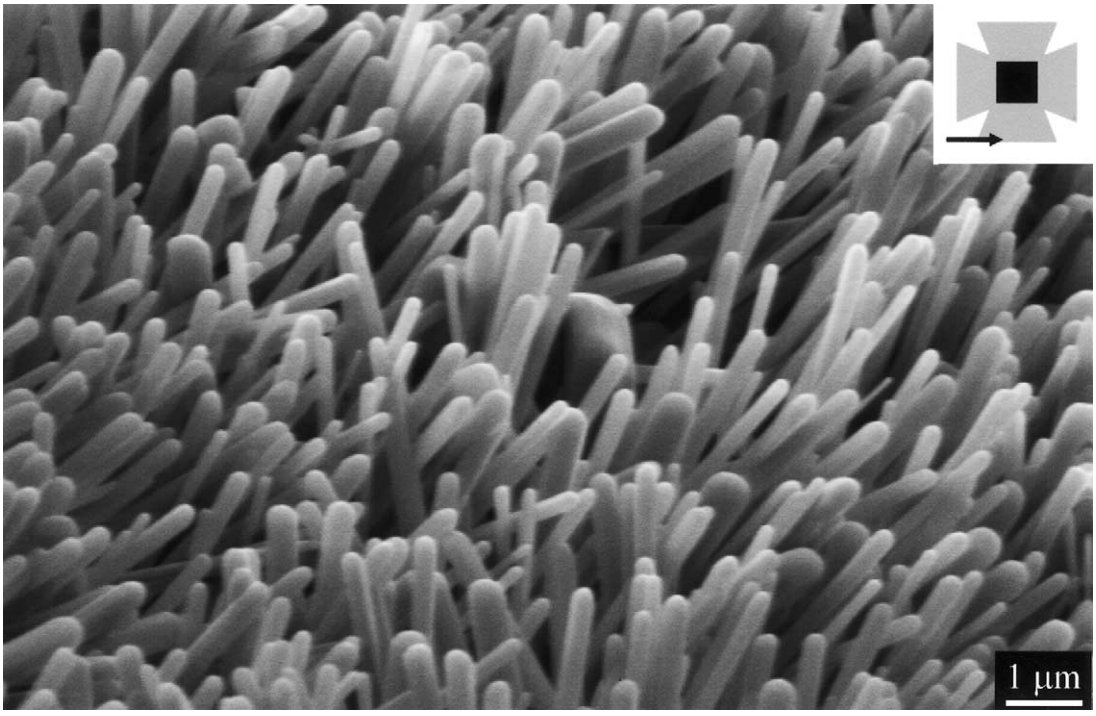

Fig. 10. SEM micrograph of the cross surface of a sample oxidized 24 h at 1350 °C.

Semi-quantitative microprobe analysis yielded also the possibility of calculating a stoichiometry of the aluminium borate crystals (Eq. (1)):

$$Al_{17.7\pm0.4}B_{2.7\pm0.2}O_{34.5\pm0.5} \quad (1)$$

EMPA-WDS line scans showed no compositional gradients within the oxide scale.

On the contrary, a variation of the morphology within the oxide scale is observed along the same direction: In the inner oxidized area, aluminium borate crystals exhibit platelet-like structure with embedded spheroidal grains of hafnia (Fig. 9), whereas towards the surface and on the surface, a needle-like structure prevails for aluminium borate crystals while hafnia grains are no more visible (Fig. 10).

4. Discussion

Depending on the oxidation temperature, two different aluminium borates can be formed. Results of XRD analysis are in good agreement with literature data[13,14] showing the presence of only the high temperature (>1000 °C) phase, $Al_{18}B_4O_{33}$ (Fig. 5).

The possible reactions for the oxidation of the starting materials can be described by the following equations:

$$HfB_2 + \tfrac{5}{2}O_2 = HfO_2 + B_2O_3 \quad (2)$$

$$AlN + \tfrac{3}{4}O_2 = \tfrac{1}{2}Al_2O_3 + \tfrac{1}{2}N_2 \quad (3)$$

$$\tfrac{1}{2}Al_2O_3 + \tfrac{1}{9}B_2O_3 = \tfrac{1}{18}Al_{18}B_4O_{33} \quad (4)$$

$$AlN + \tfrac{1}{9}B_2O_3 + \tfrac{3}{4}O_2 = \tfrac{1}{18}Al_{18}B_4O_{33} + \tfrac{1}{2}N_2 \quad (5)$$

Thermodynamic data suggest that the formation of aluminium borate is favoured over the existence of individual aluminium, boron oxides at all temperatures.

No phase diagram for the ternary Al_2O_3–B_2O_3–HfO_2 system has been found and the binary HfO_2–Al_2O_3 diagram shows no binary phase up to 1800 °C.[15] Due to the high stability of hafnia and aluminium borate in the experimental temperature range, it is possible to assume the same behaviour as in the hafnia-alumina system. Furthermore, electron probe microanalysis results showed no mixing between the two oxides. The quantitative results of EPMA-WDS yielding a non-stoichiometric composition for the aluminium borate crystals and in particular a boron deficit (Eq. (1)) must not be considered absolute values, given the difficulty of precise light-element quantitative analysis.[11]

In order to estimate the quantity of boron oxide "trapped" through the formation of aluminium borate crystals, a simple theoretical evaluation may be performed. Given the initial composition of the composite, only 42% of B_2O_3 produced by reaction (2) is needed to consume all the starting aluminium nitride, by reaction (5).

This figure along with the increasing vapour pressure value of boron oxide with temperature (Table 2), leads to the conclusion of a preferred evaporation of B_2O_3. This is in agreement with the cited non-stoichiometry but may not be considered conclusive.

Table 2
Vapour pressure for B_2O_3 [16]

Temperature (°C)	Vapour pressure (atm)
900	9.32646E−09
1000	1.88242E−07
1100	2.43622E−06
1200	2.20149E−05
1300	1.48839E−04
1400	7.9381E−04
1500	3.481101E−03

The oxidation resistance of the AlN–HfB_2 composite studied is very high up to 1100 °C with an initial fast uptake and a subsequent steady and slow mass increase (Fig. 2). This behaviour is consistent with the results previously published for the oxidation of pure HfB_2.[3] In particular, a glassy B_2O_3-rich phase embedding HfO_2 grains is observed (Fig. 6), covering the yet not reacted AlN matrix (Fig. 5). The logarithmic kinetic suggests that the oxidation of inner HfB_2 grains is becoming negligible as soon as the continuous thin glassy film of quasi-constant thickness is formed.

At 1200 °C, the initial rapid uptake is followed by a linear mass increase. Experiments carried on for up to 72 h showed no significant deviation from this linear behaviour. In this case, higher boria evaporation rates prevent the coverage of the surface by the continuous glassy film and enhance the diffusion of oxygen through the oxide film. Reaction with aluminium nitride yields to the growth of aluminium borate crystals, which denote an elongated or columnar shape (Fig. 7) in agreement with literature data.[10,13,14,17,18]

Above 1200 °C, oxidation kinetic curves assume a sigmoidal shape (Fig. 3) with the inflection point linked to the formation of a Maltese cross structure (Fig. 8). In the initial period, up to the inflection point, the reaction at the oxide–gas interface may be the limiting step. In this hypothesis, the observed rate increase originates in the augmentation of the actual surface area of the cube due to the reaction volume expansion. The surface morphology of aluminium borate crystals, which grow as vertically aligned whiskers (Fig. 10), may also contribute to the observed kinetics. In consequence, the surface layer is less protective creating a sort of pathway for incoming oxygen. In this work, no hollow aluminium borate crystal were observed (Fig. 10), unlike in oxidation of AlN–TiB_2 ceramic.[10]

Conversely, the final period after the inflection point, which is characterized by decelerating oxidation rates, is associated with the opening of the oxide scale at the sample's edges allowing a direct access of the reactive gas to the internal interface (composite/oxide), whose area decreases due to a shrinking core effect (Fig. 10).

The edges' break up may be related to the low plasticity of both oxides, aluminium borate ($T_m \sim 1950$ °C) and hafnia ($T_m \sim 2770$ °C), that prevents accommodation of growth stresses when oxide scales reach a critical thickness, which depends on the temperature (Fig. 3).

5. Conclusions

The oxidation of a hipped AlN–HfB_2 electroconductive particulate ceramic composite in oxygen produces hafnia and an aluminium borate, $Al_{18}B_4O_{33}$, as the main reaction products. The dominating mechanism to produce aluminium borate crystals was found to be the direct formation via reaction of AlN, B_2O_3 and O_2. The oxide scale has high protective properties up to 1100 °C where logarithmic isothermal kinetic are recorded. A kinetic break is present at 1200 °C, while sigmoidal oxidation kinetic curves are observed for higher temperatures, resulting from the formation of Maltese cross scale geometry due to cracking along sample edges.

Acknowledgements

This work is part of a EU funded Research Training Network on "Corrosion of ceramic matrix composites", HPRN-CT-2000-00044. The authors wish to thank Dr. Daniel Tétard (Université de Limoges, France) for HIP processing and Dr. Thomas Wenzel (Geosciences Faculty, University of Tuebingen, Germany) for microprobe analysis.

References

1. Opeka, M., Talmy, I. G., Wuchina, E., Zaykoski, J. A. and Causey, S. J., Mechanical, thermal, and oxidation properties of refractory hafnium and zirconium compounds. *J. Eur. Ceram. Soc.*, 1999, **19**, 2405–2414.
2. Wiley, D. E., Manning, W. R. and Hunter, O. J., Elastic properties of polycrystalline TiB_2, ZrB_2 and HfB_2 from room temperature to 1300 K. *J. Less Comm. Met.*, 1969, **18**, 149–157.
3. Metcalfe, A. G., Elsner, N. B., Allen, D. T., Wuchina, E., Opeka, M. and Opila, E. In *Proceedings of the Electrochemical Society*, 2000, **99**(38), 489–501.
4. Panasyuk, A. D., Lavrenko, V. A. and Korablev, S. F., High temperature oxidation of AlN–SiC ceramics. *Key Eng. Mater.*, 1997, **132–136**, 1621–1624.
5. Misirli, Z., Erkalfa, H. and Ozkan, O. T., Effect of B_2O_3 addition on the sintering of α-Al_2O_3. *Ceram. Int.*, 1996, **22**, 33–37.
6. Mazdiyasni, K. S., Ruh, R. and Hermes, E. E., Phase characterization and properties of AlN–BN composites. *Am. Ceram. Soc. Bull.*, 1985, **64**, 1149.
7. Gogotsi, Y. G., Desmaison, J., Andrievski, R. A., Baxter, D. J., Desmaison, M., Frodham, R. *et al.*, AlN-based ceramics—an alternative to Si_3N_4 and SiC in high temperature applications? *Key Eng. Mater.*, 1997, **132–136**, 1600–1603.
8. Gogotsi, Y. G. and Lavrenko, V. A., *Corrosion of High-Performance Ceramics*. Springer, Berlin, 1992.
9. Lavrenko, V. A., Panasyuk, A. D. and Smirnov, V. P., High temperature oxidation of AlN–ZrB_2 ceramics. *Key Eng. Mater.*, 1997, **132–136**, 1625–1628.
10. Schneider, S., Desmaison, M., Gogotsi, Y. G. and Desmaison, J., Oxidation behaviour of a hot isostatically pressed TiB_2–AlN composite. *Key Eng. Mater.*, 1996, **113**, 49–58.
11. Wenzel, T., Nickel, K. G., Glaser, J., Meyer, H. J., Eyidi, D. and Eibl, O., Electron probe micro-analysis of MgB compounds: stoichiometry

and heterogeneity of superconductors. *Phys. Stat. Sol. (a)*, 2003, **198**, 374–386.
12. Nickel, K. G. and Gogotsi, Y. G. In *Handbook of Ceramic Hard Materials, Vol 1*, ed. R. Riedel. Wiley-VCH Verlag, Weinheim, 2000, pp. 140–182.
13. Ray, S. P., Preparation and characterization of aluminium borate. *J. Am. Ceram. Soc.*, 1996, **75**, 2605–2609.
14. Schneider, S., Desmaison, M., Richter, G., Porz, F. and Gault, C., Thermomechanical behaviour of TiB_2–AlN composites. *Key Eng. Mater.*, 1997, **132–136**, 524–527.
15. Lopato, L. M., Shevchenko, A. V. and Gerasimyuk, G. I. In *Phase Diagrams for Ceramics*, ed. A.C. Society. 1976, p. 146.
16. *Handbook of Chemistry and Physics (73rd ed.)*. CRC-Press, 1992–1993.
17. Tampieri, A. and Bellosi, A., Oxidation of monolithic TiB_2 and Al_2O_3–TiB_2 composites. *J. Mater. Sci.*, 1993, **28**, 649–653.
18. Cheng, C., Ding, X. X., Shi, F. J., Cheng, Y., Huang, X. T., Qi, S. R. *et al.*, Preparation of aluminum borate nanowires. *J. Cryst. Growth*, 2004, **263**, 600–604.